

Marcos Nicolás Gallo · Susana Beatriz Vinzon

## Generation of overtides and compound tides in Amazon estuary

Received: 4 April 2005 / Accepted: 28 May 2005 / Published online: 30 August 2005  
© Springer-Verlag 2005

**Abstract** Tidal propagation in estuaries is affected by friction and fresh water discharge, besides changes in the depth and morphology of the channel. Main distortions imply variations in the mean water level and asymmetry. Tidal asymmetry can be important as a mechanism for sediment accumulation and turbidity maximum formation in estuaries, while mean water level changes can affect navigation depths. Data from several gauges stations from the Amazon estuary and the adjacent coast were analyzed and a 2DH hydrodynamic model was configured in a domain covering the continental shelf up to the last section of the river where the tidal signature is observed. Based on data, theoretical and numerical results, the various influences in the generation of estuarine harmonics are presented, including that of fresh water discharge. It is shown that the main overtide,  $M_4$ , derived from the most important astronomic component in the Amazon estuary,  $M_2$ , is responsible for the tidal wave asymmetry. This harmonic has its maximum amplitude at the mouth, where minimum depths are found, and then decreases while tide propagates inside the estuary. Also, the numerical results show that the discharge does not affect water level asymmetry; however, the Amazon river discharge plays an important role in the behavior of the horizontal tide. The main compound tide in Amazon estuary,  $M_{sf}$ , generated from the combination of the  $M_2$  and  $S_2$ , can be strong enough to provoke neap low waters lower than spring ones. The results show this component increasing while going upstream in the estuary, reaching a maximum and then slightly decaying.

**Keywords** Tidal propagation · Tidal asymmetry · Shallow-water harmonics · Amazon estuary

### 1 Introduction

Tidal propagation in estuaries is affected by friction and fresh water discharge (Dronkers 1964; Godin 1985, 1999), besides changes in depths and the morphology of the channel (Dronkers 1964; Ippen and Harleman 1966; Shetye and Gouveia 1992; Friedrichs and Aubrey 1994; Lanzoni and Seminara 1998), which implies variations in the mean water level and asymmetry of the tidal wave.

Tidal asymmetry is explained through the generation of overtides (Dronkers 1964; Pugh 1987; Dyer 1997). In the Amazon estuary, the presence of the  $M_4$  harmonic is the main cause of wave distortion or modification (Gallo 2004), causing disparities in the rising and falling times. This special feature is important, in some cases, as a mechanism for sediment accumulation and turbidity maximum formation in estuaries.

In the upper part of the Amazon estuary, modifications in the mean water level due to the generation of compound tides may become more important than changes imposed by the main astronomical tide, which may affect the navigation depths. This feature has been reported in the upper Saint Lawrence river (Godin 1999). For building the navigation charts, for instance, the criteria for establishing the navigation depth is the minimum occurring during the spring low water stage. However, in the estuary, neap low water levels can be lower than the spring levels one due to this tidal compound (Speer and Aubrey 1985; Gallo 2004).

The Amazon tide is semi-diurnal, being  $M_2$  (12.4 h) and  $S_2$  (12 h), the most important astronomic components. Consequently, the main overtide is the  $M_4$  (6.2 h) and the main compound tide is  $M_{sf}$  (354.4 h), from the combination of  $M_2$  and  $S_2$  (Gallo 2004). The aim of this work is to understand different mechanisms affecting the generation of these shallow water harmonics with

Responsible Editor: Alejandro Souza

M. N. Gallo (✉) · S. B. Vinzon  
Coastal and Oceanographic Engineering Area,  
Ocean Engineering Program/COPPE,  
Federal University of Rio de Janeiro,  
CT C203 Cx Po 68508, 21945-970,  
Rio de Janeiro, Brasil  
E-mail: marcosgallo@peno.coppe.ufrj.br  
Tel.: +55-21-25628811  
Fax: +55-21-25628748

reference to the Amazon estuary. Considering available tidal records, the amplitude of the main astronomic components, overtides and compound tides are analyzed in regard to their spatial location and respective forcings. A 2DH hydrodynamic model was configured and calibrated in order to help in the analysis and to consider the effects of river discharge, which cannot be analyzed from the scarce data.

## 2 Description of the area

Considering an estuary as being an area where the sea and river encounter, the Amazon estuary extends from the continental shelf, where fresh and ocean waters mix, up to Óbidos city, where the tide propagates. The Amazon estuary is a very energetic ambient, where the fresh water discharge and oceanic tides are the main responsible agents for the water level oscillation. The mean fluvial discharge to Atlantic ocean is about 170,000 m<sup>3</sup>/s (at Óbidos city), with maximum and minimum values of 270,000 and 60,000 m<sup>3</sup>/s (ANA 2003), respectively. At the Amazon mouth, the main astronomic components are the M<sub>2</sub>, S<sub>2</sub>, N<sub>2</sub> (semi-diurnals), K<sub>1</sub> and O<sub>1</sub> (diurnals) with amplitudes of ~140, 30, 20, 10 and 5 cm, respectively. The estuary is classified as macrotidal (Dyer 1997), with a tidal range between 4 and 6 m, and as semi-diurnal (Pugh 1987), with a wave shape relationship (the quotient of the diurnals to semi-diurnals harmonics) equal to 0.1.

Figure 1 shows the study area, bathymetry and a longitudinal bottom profile. The upper reach (0–500 km) has a mean slope of 2×10<sup>-5</sup>, with a mean depth of ~30 m. When the river branches, the slope is about

zero and depths decrease to about 20 m in both channels. At the mouth, depths are about 10 m. The continental shelf extends up to 100 m depth with a slope of about 2×10<sup>-4</sup>. Sand is the dominant bottom sediment in the upper part of the estuary up to the mouth, and at the southern part of the Amazon continental shelf. Thick mud deposits have been recorded (AmasSeds 1990) in the front and the north of the mouth, which has been shown, is important for tidal propagation (Gabioux et al. 2005).

## 3 M<sub>4</sub> and M<sub>SF</sub> generation: theoretical analysis

Tidal propagation can be obtained from the following one dimensional governing equations (Dronkers 1964):

$$\frac{\partial u}{\partial t} + u \frac{\partial u}{\partial x} = -g \frac{\partial z}{\partial x} - \frac{g}{C^2(H+z)} u|u| \quad (1)$$

$$\frac{\partial}{\partial x} [(H+z)u] = -\frac{\partial z}{\partial t} \quad (2)$$

where  $H$  is the depth at the  $x$  location,  $C$  is the Chézy friction coefficient, and  $g$  is the gravity acceleration. In the non-linear terms appear the products of two unknowns,  $u$  (velocity) and/or  $z$  (level):

1. Friction term:  $\frac{g}{C^2(H+z)} u|u| \approx \frac{g}{C^2} \left( \frac{u|u|}{H} - \frac{z}{H} \frac{u|u|}{H} \right)$  (Godin and Martinez 1994),  $u|u|$  being more significant, since in general  $\frac{z}{H} < 1$ .
2. Advective term:  $u \frac{\partial u}{\partial x} = \frac{\partial}{\partial x} \left( \frac{u^2}{2} \right)$ ;
3. Non-linear flux of continuity:  $\frac{\partial}{\partial x} (zu)$ .

**Fig. 1** Amazon estuary, bathymetry (continuous lines) and mud-sand roughness distribution. A longitudinal bottom profile, considered the North channel, is also included in the up left square. Source: navigation charts (DHN, Brazilian Navy/Directorate of Hydrography and Navigation)

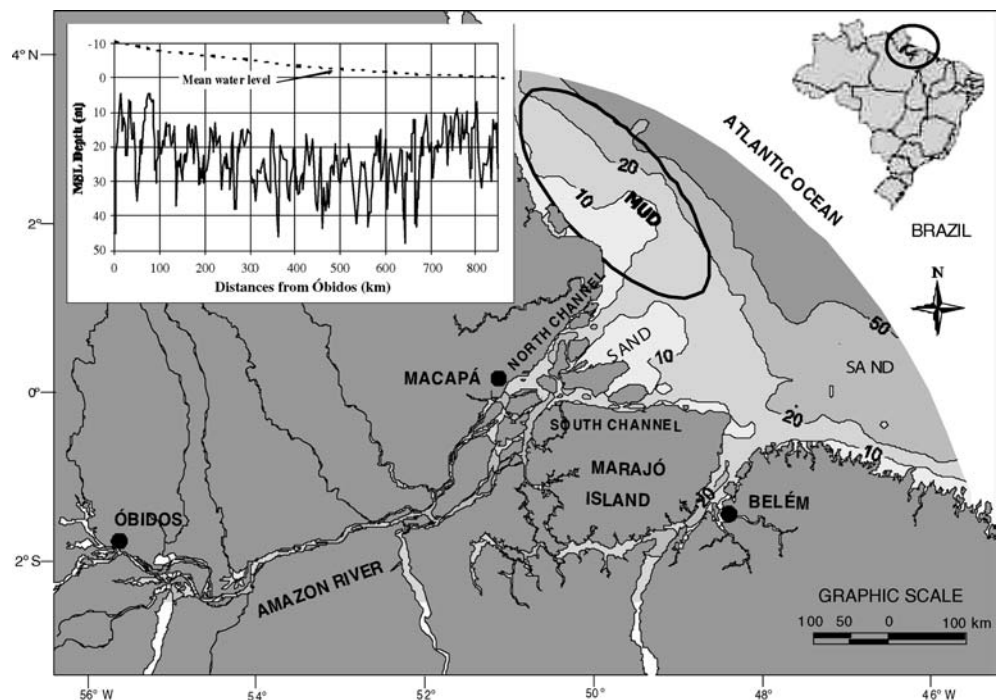


**Table 1**  $M_4$  and  $M_{sf}$  relative amplitudes obtained from the theoretical analysis of the nonlinear terms: friction, advection, and continuity

| Harmonic | Frequency                        | Relative amplitudes |                       |                       |
|----------|----------------------------------|---------------------|-----------------------|-----------------------|
|          |                                  | Friction            | Advection (ADV)       | Continuity (CONT)     |
| $M_4$    | $\cos [2\sigma_1 t]$             | $a_0 a_1^2$         | $\frac{1}{4} a_1^2$   | $\frac{1}{2} a_1 b_1$ |
| $M_{sf}$ | $\cos [(\sigma_1 - \sigma_2) t]$ | $2a_0 a_1 a_2$      | $\frac{1}{2} a_1 a_2$ | $a_1 b_2 + b_1 a_2$   |

Three principal components were considered:  $\theta$  (fluvial discharge),  $\sigma_1 (M_2)$  and  $\sigma_2 (S_2)$ . Amplitudes normalized by the square of the maximum velocity (for the friction,  $\frac{u|u|}{U^2}$  and advective terms,  $\frac{u}{U} \frac{\partial u}{\partial x}$ ) and by the product of the maximum water level range and maximum velocity (for the continuity term,  $\frac{\partial z}{\partial x} \frac{zU}{U}$ )

The water level and velocity will be considered as a sum of permanent and transient parts, regarding the river discharge ( $\theta$ ) and  $N$  tidal harmonics ( $\sigma_j$  frequencies,  $j=1$  to  $N$ ), respectively.

$$z(x, t) = z_0(x) + \sum_{j=1}^N z_j(x) \cos(\sigma_j t) \quad (3)$$

$$u(x, t) = -u_0(x) + \sum_{j=1}^N u_j(x) \cos(\sigma_j t) \quad (4)$$

The product  $u|u|$  is considered as a sum of two odd terms of  $u, u|u| \approx (0.35u + 0.71u^3)$  according to Godin and Martinez (1994); Godin (1999); Gallo (2004).

Replacing Eqs. 3 and 4 in the non-linear terms listed above, new harmonics will be generated with frequencies which are products, sums or differences of the original ones. The interaction between the generated and original harmonics is not considered in this analysis. Also, phase differences are not accounted for.

The resulting harmonics generated through the non-linear terms were normalized by the square of the maximum velocity (for the friction and advective terms) and by the product of the maximum velocity and maximum water level range (for the continuity term). Table 1 shows the relative amplitudes for the  $M_4$  and  $M_{sf}$  harmonics, obtained from this analysis. These are specific cases of the amplitudes found in previous works (Godin and Gutierrez 1996; Godin 1999).

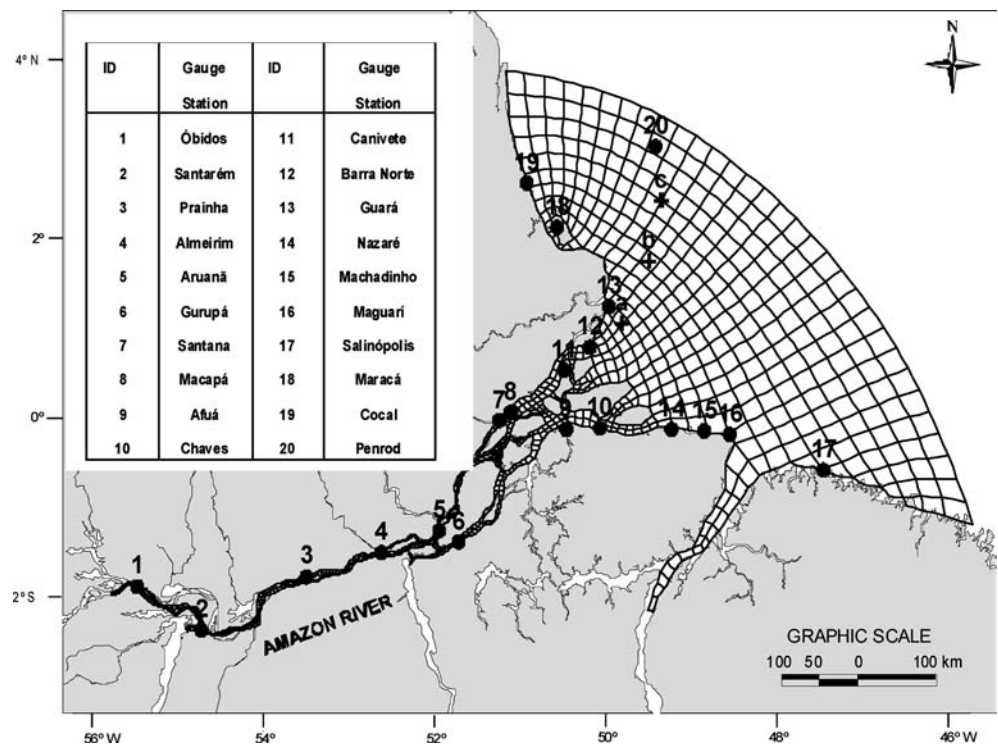
Thus, knowing the amplitudes (for velocities,  $a_j$ , and levels,  $b_j$ ) of the original components at each location in the estuary, it is possible to infer the contribution of each non-linear term to the new generated harmonics.

#### 4 Data analysis and tidal propagation model

The harmonic analysis was applied both for measured and calculated water levels. The component amplitudes were obtained using the program T\_TIDE (Pawlowicz et al. 2002). Measured and simulated series were 30 days long.

The 2DH module of the SisBAHIA hydrodynamics model, <http://www.sisbahia.coppe.ufrj.br> (Rosman 1987, 2001), was configured and calibrated, aiming to help in the analysis through the numerical inspection of

**Fig. 2** Gauge stations analyzed (1–20, with black circles) and the numerical mesh. With black cross are indicated three intermediate points (a, b and c) in the simulations. Source data: HiBAm Project, Hydrology and Geochemistry of the Amazon Basin (stations 1–7) and DHN, Brazilian Navy/Directorate of Hydrography and Navigation (stations 8–20)



the contribution of the different non linear terms, with emphasis in the effect of the river discharge, which could not be analyzed from the scarce data. Figure 2 shows the numerical mesh and the location of the tidal gauge stations. The model extends over 1,200 km, from the upper limit, 100 km upstream of Óbidos city, up to the continental break. The mesh has 1,022 finite elements, with a resolution of 15 km at the continental shelf, 12 km at the mouth area and 1 km in the upper estuary. A time step for the simulations was 200 s, given a maximum Courant number of 8 and a mean of 1.75. The bottom friction in the sand regions considered the values of the roughness recommended by Abbot and Basco (1989) for bed with sand transportation,  $O(10^{-2}$  m). In the muddy area over the shelf (see Fig. 1), the strong interaction between the high concentration fine sediments and hydrodynamics was considered following Gabioux et al. (2005). In this region, roughness values of  $O(10^{-7}-10^{-9}$  m) were considered. The fluvial boundary condition was established considering a constant discharge: the mean river discharge and a zero value in order to highlight the effect of this forcing on the generation of tidal harmonics. At the sea boundary, the two main astronomical tidal constituents  $M_2$  and  $S_2$  were prescribed, which explains about 70 and 85% of its amplitude. The amplitude and phase were taken from data reported in the literature (Beardsley et al. 1995; FEMAR 2000).

The model was calibrated with the main astronomical components obtained from the tidal records from the 20-gauge stations, as shown in Fig. 2. This data set was mainly collected in short periods of 30 days, during the months of March or September when the river discharge was approximately at its mean value, considered as the fluvial boundary condition. Forty five days were simulated and the first 15 days were discarded to avoid the influence of the initial conditions on the results.

**Fig. 3** Tidal amplitudes for the main astronomic components,  $M_2$  (a) and  $S_2$  (b), for the stations along the coast. Measured (symbols) and modeled (lines) results

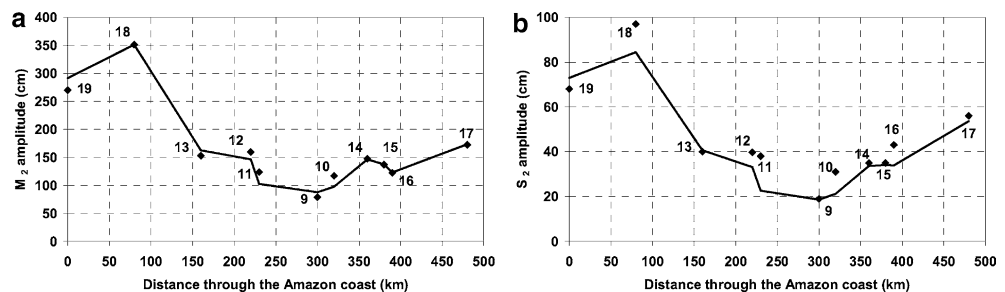
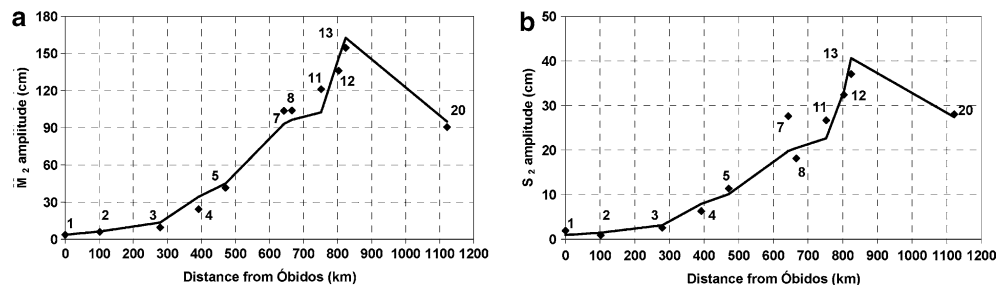


**Fig. 4** Tidal amplitudes for the main astronomic components,  $M_2$  (a) and  $S_2$  (b), for the stations along the longitudinal profile. Measured (symbols) and modeled (lines) results



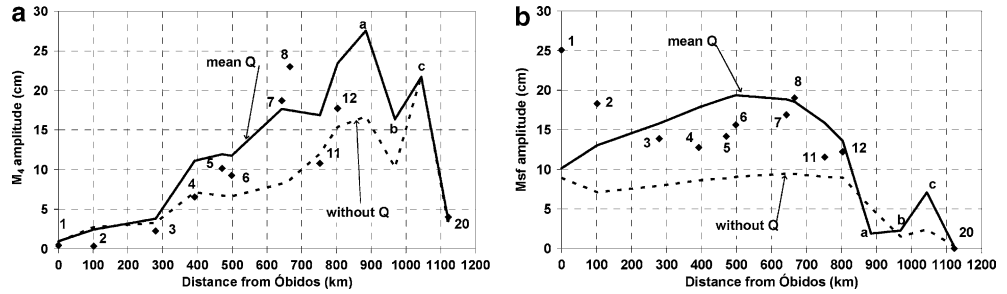
Figures 3 and 4 show the comparison of data and numerical results for the amplitudes of the main astronomic components,  $M_2$  and  $S_2$ , for the stations along the coast (Fig. 3), from north to south, and for the stations along a longitudinal transect from Óbidos city up to the continental break (Fig. 4). Notice the difference in the scales for both Figures. The amplification observed in the coastal area is due to the resonant effect at the embayment (Beardsley et al. 1995). This effect is also important at the mouth. The reduction in the friction due to the mud deposit (Gabioux et al. 2005) helps to keep tidal amplitudes high at the north area. Once propagating in the estuary channels, the astronomical tidal amplitudes decrease progressively. As can be seen in Figs. 3 and 4, the fit between model and data is good, with amplitude errors lower than 10%, which was considered satisfactory for the purposes of in this work. The fitting of the model in terms of phase was also considered good, but not presented here. Errors of the order of  $5^\circ$  were observed in the lower estuary and the northern coast, with more severe differences in the upper estuary and southern coast (of the order of  $30^\circ$ ).

## 5 Results

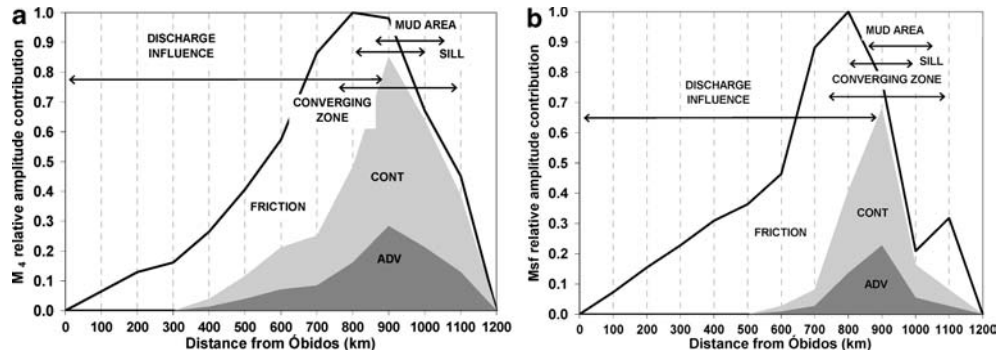
### 5.1 The contributions of the river discharge, depth, roughness and estuary convergent shape to the shallow water harmonics

Figure 5 shows a comparison between the measured and simulated amplitudes for the two considered main shallow water harmonics,  $M_4$  and  $M_{sf}$ . Modeled values fit well the measured ones, except for the  $M_{sf}$  harmonic in the upper part of the estuary where the monthly changes of the river discharge are much stronger than in the lower part of the estuary. This effect is not accounted for in the

**Fig. 5** Tidal amplitudes for the main shallow water components,  $M_4$  (a) and  $M_{sf}$  (b), along the longitudinal profile. Measured (symbols) and modeled (lines) results, including the zero discharge simulation (dash line)



**Fig. 6** Contributions from the friction, advection ( $ADV$ ) and continuity ( $CONT$ ) terms to the  $M_4$  (a) and  $M_{sf}$  (b) amplitudes, relatives to the maximum observed value in the estuary. Theoretical analysis based on numerical results with the mean discharge



constant discharge simulations. In most of the stations the differences between observed and simulated amplitudes was about 5–10 cm. The results for zero discharge are also included in Fig. 5. In order to have a more continuous picture of the tidal propagation behavior, three intermediate points over the shelf are included (a, b and c, see Fig. 2), considering only the model results.

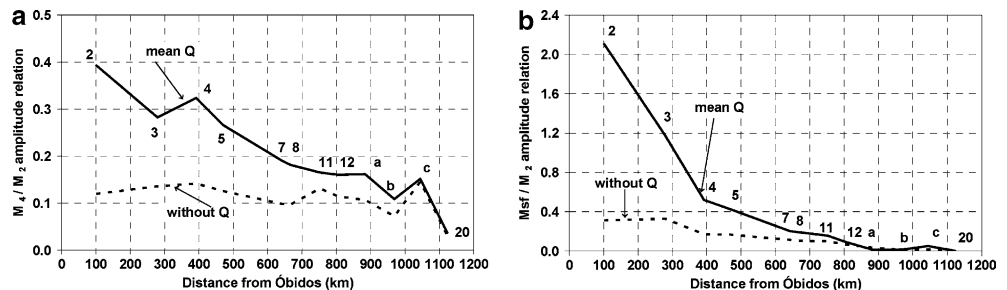
With the principal component amplitudes (discharge,  $M_2$  and  $S_2$ ), obtained from numerical results at each location, their contribution to the amplitude of the two shallow water harmonics is calculated for each non-linear term as expressed in Table 1. The normalizing scales were the local depth,  $H$ , the roughness,  $C$ , and the maximum tidal range,  $Z$ , at each station, and the wavelength ( $O(10^2)$  km for  $M_4$  and  $O(10^3)$  km for  $M_{sf}$ ), for  $\Delta x$ , and the time frequency ( $\sigma_{M_4} = 2.8 \times 10^{-4}/s$  for  $M_4$  and  $\sigma_{M_{sf}} = 5 \times 10^{-6}/s$  for  $M_{sf}$ ), for  $\Delta t$ . The contributions from each non-linear terms are showed in Fig. 6. The friction term provides the main contribution for both harmonics over the upper part of the estuary up to the mouth (from 0 to 800 km), as could be expected from the strong influence of the river discharge. The transition from mud to sand, over the shelf, occurs approximately in the 1,000–1,100 km, and the friction

again becomes important for  $M_{sf}$  amplitude, with a new peak. Continuity and advection non linear terms are preponderant at the mouth, where the lower depths and converging shape of the estuary occur. These two terms have a stronger influence on the  $M_4$ .

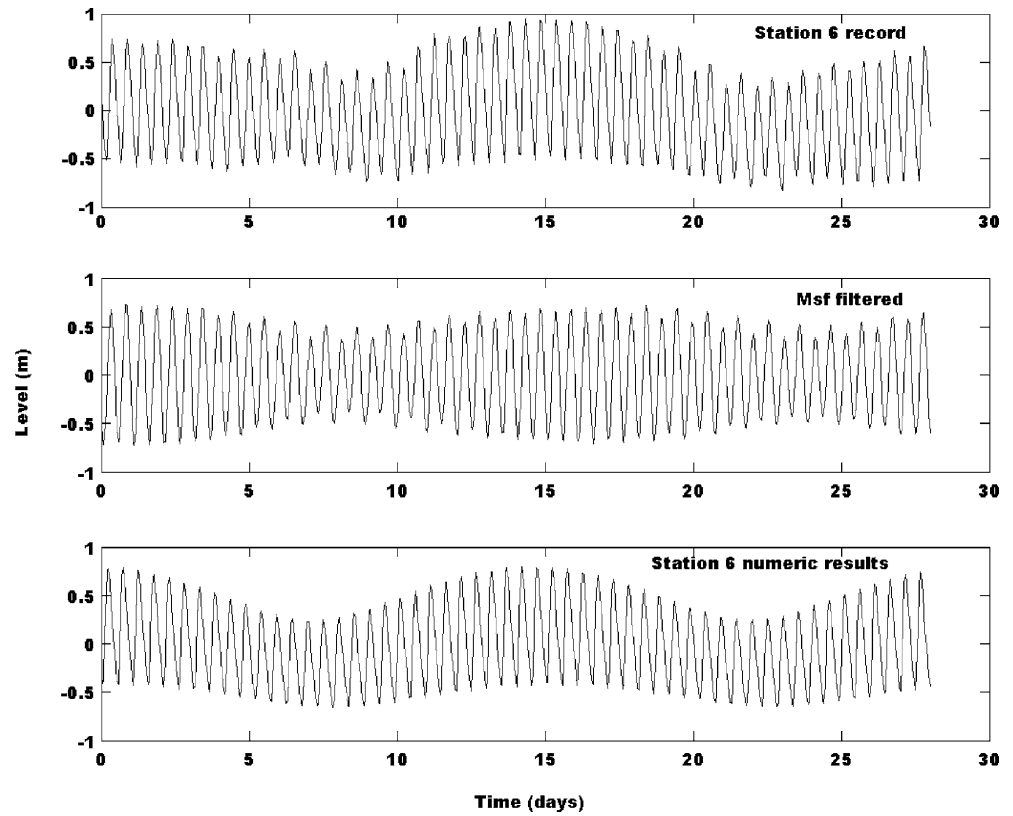
The influence of the river discharge on the  $M_4$  and  $M_{sf}$  can be seen in Fig. 5, comparing both simulations, for the mean and zero river discharge. It is interesting to compare Figs. 5 and 6. In agreement with the theoretical results depicted in Figs. 5 and 6, shows that the river discharge represents about the 40% of the  $M_4$  amplitude and 50% of the  $M_{sf}$  one. The continuity and advective non-linear terms do not depend on the river discharge, then, the zero discharge line must follow the trend of these terms. This happens for the  $M_4$ . For the  $M_{sf}$  harmonic, however, the zero discharge line does not follow the continuity and advective contributions. This is explained by the fact that the  $M_{sf}$  is a long wave which propagates beyond the original components. The upstream propagation is not accounted for by the theory, and, consequently, the results are masked in some extent.

Figure 7 shows the influence of the river discharge in the growth of the shallow water harmonics, relative to the  $M_2$  amplitude. The energy transfer from the  $M_2$  to its

**Fig. 7** Effect of Amazon river discharge on the  $M_4$  (a) and  $M_{sf}$  (b) amplitudes. Numerical results with the mean discharge (solid line) and zero discharge (dash line)



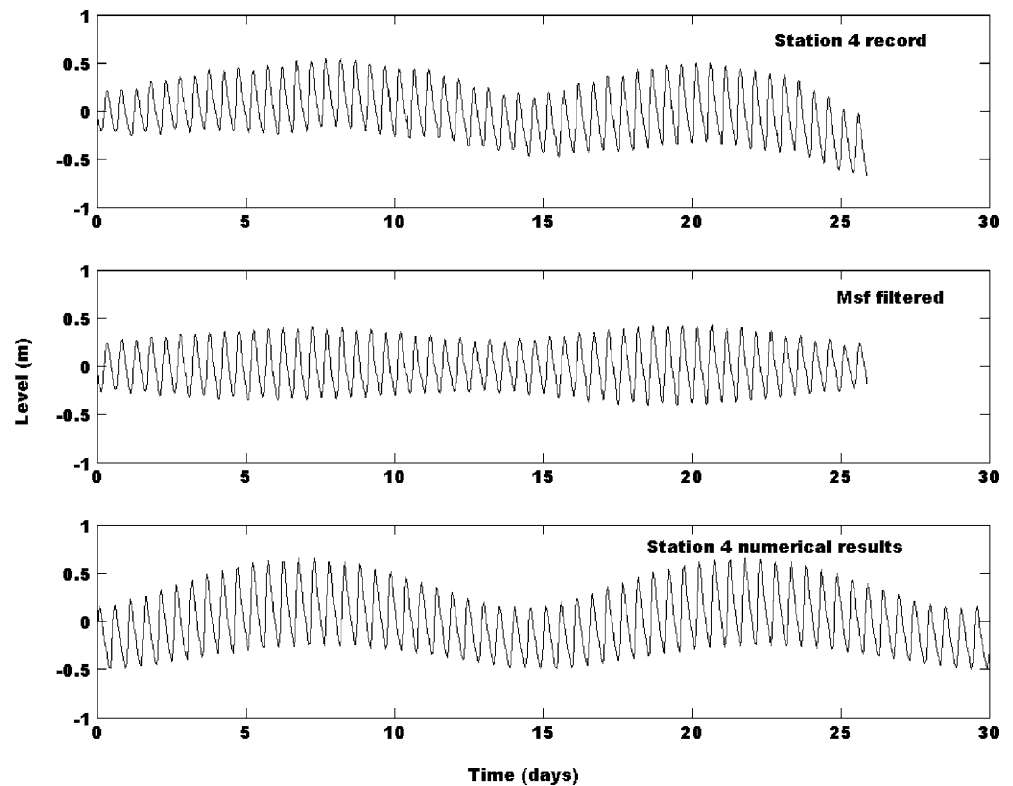
**Fig. 8** Water level in Gurupá (gauge 6), measured, filtered M<sub>sf</sub> component and simulated with the mean discharge



first harmonic,  $M_4$ , varies from 10 to 40% of the  $M_2$ , for the mean river discharge, and remains almost constant (10% of  $M_2$ ) for the zero discharge. In the upper part of the estuary and disregarding the river discharge,  $M_{sf}$

amplitudes increase beyond the amplitude of the original component,  $M_2$ . This is also explained by the further upstream propagation of longer waves.

**Fig. 9** Water level in Almeirim (gauge 4), measured, filtered M<sub>sf</sub> component and simulated with the mean discharge



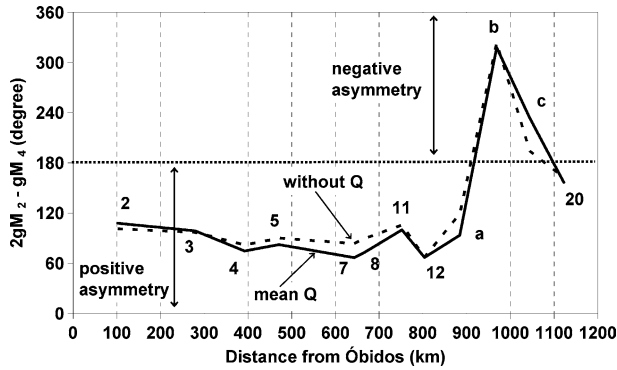


**Fig. 10** Asymmetry within the estuary. Numerical results with the mean discharge (solid line) and zero discharge (dash line)

## 5.2 Msf and $M_4$ effects on Amazon tides

The effect of the Msf can be observed for example in the Gurupá station (station 6 in Fig. 2). Figure 8 presents the measurements at this station during four weeks compared to the same data after filtering the Msf component. Also, in the same figure, numerical results are presented for the same station, with the mean river discharge. The Msf is in phase with the spring-neap cycles. At this station the amplitude of Msf is about 40% of the  $M_2$  amplitude and the lowering of the neap low water level with respect to the spring one, is already noticeable. In the upper part of the estuary, where  $M_2$  and  $S_2$  are strongly damped and the spring neap cycle is not evident any more, the Msf modulates the water level,

as shown for example for the Almeirim station (station 4 in the Fig. 2) in Fig. 9.

The relative phase of the  $M_4$  to  $M_2$ , expressed as  $2\Phi(M_2) - \Phi(M_4)$  (Speer and Aubrey 1985), is the main factor controlling the tidal wave asymmetry. Regarding the water levels, or the vertical tide, for  $0 < 2\Phi(M_2) - \Phi(M_4) < 180^\circ$ , the asymmetry is positive and the rising time will be shorter than the falling one, while for  $180^\circ < 2\Phi(M_2) - \Phi(M_4) < 360^\circ$ , the opposite occurs. Figure 10 shows this phase relationship for the Amazon model results, calculated from the water level components,  $M_4$  and  $M_2$ , obtained through the harmonic analysis of the numerical results, for the mean and zero discharges. Over the continental shelf, where the strong convergence of the tide is observed, the asymmetry is negative, while in the inner part, where the energy dissipation due to friction is predominant, from the mouth up to the limit of tidal propagation, the asymmetry is positive. This behavior was also observed by Lanzoni and Seminara (1998), for the analysis of the observed tidal and geometric properties of various tidal estuaries.

It is noticeable in Fig. 10 that the water level asymmetry is not affected by the changes in the river discharge. However, regarding the behavior of the tidal velocities, also called the horizontal tide, the river discharge plays an important role. In the literature, estuaries with positive asymmetry for the vertical tide are usually referred to as flood dominated estuaries (Shetye and Gouveia 1992; Friedrichs and Aubrey 1994), and estuaries with negative asymmetry as ebb dominated estuaries, considering the fact that the shorter rising or

**Fig. 11** Asymmetry in water levels and velocities, negative (a) and positive (b). Numerical results with the zero discharge

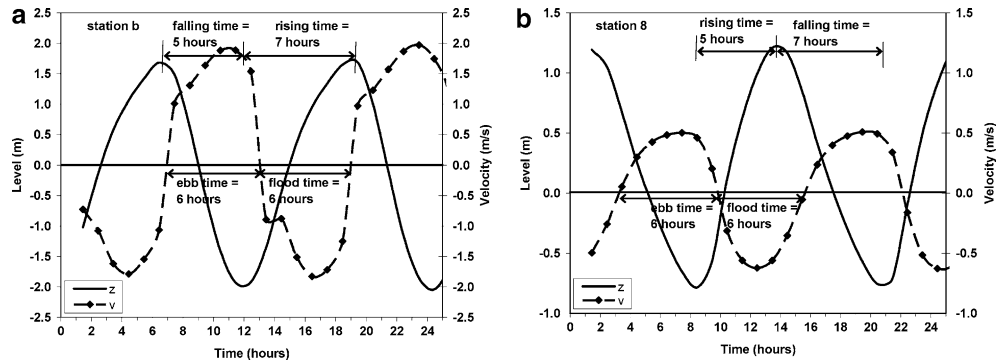
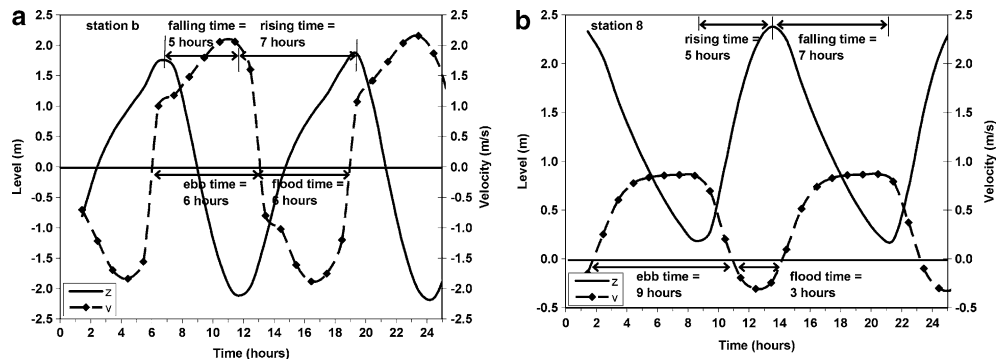


**Fig. 12** Asymmetry in water levels and velocities, negative (a) and positive (b). Numerical results with the mean discharge



falling time, would carry out stronger flows during flood or ebb, respectively. This would be the case for a zero river discharge in the estuary, as shown in Fig. 11 for stations b and 8 (see Fig. 2 for locations), representing both cases, the negative and positive asymmetry, respectively. For the case with river discharge, its flow may strongly affect this pattern, as can be seen from the simulation results presented in Fig. 12, for these stations. At the station b, where the effect of the river discharge is weak, with negative asymmetry, there is a slight increase in the ebb current with respect to the zero discharge case. At the station 8, with strong fluvial influence and with positive asymmetry reflected in the rising time being 2 h shorter than the falling time the maximum flood velocity is only about 30% of the maximum ebb velocity.

## 6 Conclusion

Three zones can be observed in the Amazon estuary. A zone where the main astronomic compounds prevail near the mouth and over the continental shelf, an intermediate zone, where the shallow water components are strong, and an upper zone where the compound tide,  $M_{sf}$ , is preponderant. Along the estuary, the contributions of the three non-linear terms, the friction, advection and continuity, for the two main shallow water harmonics,  $M_4$  and  $M_{sf}$ , were identified.

The friction term provides the main contribution for shallow water harmonics over the upper part of the estuary up to the mouth, as could be expected due to the strong influence of the river discharge. Continuity and advection non-linear terms are preponderant at the mouth, where lower depths and the converging shape of the estuary occur. The numerical results show the  $M_{sf}$  increasing while going upstream in the estuary, reaching a maximum and then decaying. The main overtide,  $M_4$ , has its maximum amplitude at the mouth, where the  $M_2$  is maximum and where the minimum depths are found, decreasing while the tide propagates inside the estuary. Its decay is stronger than for  $M_{sf}$ , according to what would be expected from a shorter period harmonic.

The main compound tide in Amazon estuary,  $M_{sf}$ , modulates the water level and can be strong enough to cause neap low water to be lower than spring ones.

Water level asymmetry is not affected by the changes in the Amazon river discharge. However, regarding the behavior of the horizontal tide, the river discharge plays an important role. Positive water level asymmetry, with shorter rising times than falling ones, in estuaries with an strong fluvial influence such as Amazon river, does not mean flood-dominated estuaries. Numerical results at the mouth of the Amazon estuary show that having a strong difference between the rise and fall of the water level in 2 h, does not result in stronger currents during flood. In this case, from the numerical results, maximum ebb currents are higher than the corresponding maxi-

mum flood currents. In fact, fine sediments accumulate out of the mouth and over the continental shelf as reported in the literature.

**Acknowledgements** The authors express their gratitude to the DHN (Brazilian Navy/Directorate of Hydrography and Navigation) and the HiBAm Project (Hydrology and Geochemistry of the Amazon Basin) for the tide data analyzed in this work and to Adriana Dantas Medeiros and Mariela Gabioux for their help with the model implementation. The first author was supported by a scholarship from CAPES Foundation (Ministry of Education).

## References

- Abbot MB, Basco R (1989) Computational fluid mechanics. An introduction for engineering. Longman Group UK Limited, Harlow
- AmasSeds (1990) A multidisciplinary Amazon shelf sediment study, EOS. Trans Am Geophys Union 71(45):1771–1777
- ANA, National Water Agency, Brazil (2003) <http://hidro-web.ana.gov.br/HidroWeb/HidroWeb.asp>
- Beardsley RC, Candela J, Limeburner R, Geyer WR, Lentz SJ, Castro BM, Cacchione D, Carneiro N (1995) The  $M_2$  tide on the Amazon shelf. J Geophys Res 100(C2):2283–2319
- Dronkers JJ (1964) Tidal computation in rivers and coastal waters. North-Holland, New York
- Dyer KR (1997) Estuaries. A physical introduction. Wiley, London
- FEMAR, Fundação de Estudos do Mar, Brazil (2000) Catalogo de estações maregráficas Brasileiras. FEMAR (eds)
- Friedrichs CT, Aubrey DG (1994) Tidal propagation in strongly convergent channels. J Geophys Res 99:3321–3336
- Gabioux M, Vinzon S, Paiva AM (2005) Tidal propagation over fluid mud layers on Amazon shelf. Contin Shelf Res 25:113–125
- Gallo MN (2004) A influência da vazão fluvial sobre a propagação da maré no estuário do rio Amazonas. MSc Thesis, University of Rio de Janeiro, Brazil
- Godin G (1985) Modification of river tides by the discharge. J Waterway Port Coastal Ocean Eng 111(2):257–274
- Godin G (1999) The propagation of tides up rivers with special considerations on the upper Saint-Lawrence river. Estuarine Coast Shelf Sci 48:307–324
- Godin G, Gutierrez G (1996) Non-linear effects in the tide of the Bay of Fundy. Contin Shelf Res 5(3):379–402
- Godin G, Martinez A (1994) Numerical experiments to investigate the effects of quadratic friction on the propagation of tides in a channel. Contin Shelf Res 14(7/8):723–748
- Ippen AP, Harleman DRF (1966) Tidal dynamics in estuaries. In: Ippen AP (ed) Estuary and coastline hydrodynamics, Mc Graw Hill Book, Chap 10. pp 493–545
- Lanzoni S, Seminara G (1998) On tide propagation in convergent estuaries. J Geophys Res 103(C13):30793–30812
- Pawlowicz R, Beardsley B, Lentz S (2002) Classical tidal harmonic analysis including error estimates in MATLAB using T\_TIDE. Comp Geosci 28:929–937
- Pugh DT (1987) Tides, surges and mean sea level. Wiley, London
- Rosman PCC (1987) Modeling shallow water bodies via filtering techniques. PhD Thesis. Department of Civil Engineering, Massachusetts Institute of Technology, USA
- Rosman PCC (2001) Um sistema computacional de hidrodinâmica ambiental. In: Vieira da Silva RC (ed) Métodos numéricos em recursos hídricos, 5. Associação Brasileira de Recursos Hídricos, Brazil, pp 1–161
- Shetye SR, Gouveia AD (1992) On the role of geometry of cross-section in generating flood dominance in shallow estuaries. Estuarine Coast Shelf Sci 35:113–126
- Speer PE, Aubrey DG (1985) A study of non-linear tidal propagation in shallow inlet/estuarine systems, II: Theory. Estuarine Coast Shelf Sci 21:207–224